Egypt. J. Chem. **Vol. 68**, No. 12 pp. 479 - 488 (2025)

Egyptian Journal of Chemistry

http://ejchem.journals.ekb.eg/

In vitro Antibacterial and Antibiofilm Activity of Isolated Compounds from *Eriobotrya japonica* Leaves against *Proteus mirabilis*

Hanim A. Youssef [1]*, Dawood Hosni Dawood[1], Engy Elekhnawy[2], Mostafa I. Sanad[1], Safaa M. Ali [1], Amal F. Soliman[3]

[1]*Agricultural Chemistry Department, Faculty of Agriculture, Mansoura University, Mansoura 35516, Egypt*

[2] *Pharmaceutical Microbiology Department, Faculty of Pharmacy, Tanta University, Tanta 31527, Egypt*

[3] *Pharmacognosy Department, Faculty of Pharmacy, Mansoura University, Mansoura 35516, Egypt*

Abstract

Loquat (*Eriobotrya japonica*) is a perennial tree, commonly grown as an ornamental plant and is known for its sweet edible fruits. Considering the traditional uses of medicinal plants, the aim of this study is the evaluation of the antibacterial action of isolated compounds from *Eriobotrya japonica* leaves. Six compounds were identified, including oleanolic acid (**1**), corosolic acid (**2**), *trans*-cinnamic acid (**3**), *trans*-sinapic acid (**4**), fisetin (**5**), and rutin (**6**). For the first time compound **5** was identified in this plant. The antibacterial effect of the two major compounds **1** and **6** was examined against *Proteus mirabilis* by applying the agar well diffusion method. Their minimum inhibitory concentrations (MICs) were then detected using broth microdilution assay. Rutin and oleanolic acid revealed MICs values ranging from 32 to 128 µg/mL and 512 to 2048 µg/mL, respectively. In addition, the antibiofilm action of the tested compounds was elucidated by crystal violet assay. Rutin exhibited antibiofilm activity, reducing the number of strong and moderate biofilm-forming isolates from 76.92% to 23.08%. Molecular analysis revealed that rutin downregulated *mrpA, pmfA, and luxS* gene expression in biofilm-forming *P. mirabilis* isolates. Further research is needed to explore the clinical implications of rutin.

Keywords: Eriobotrya japonica, NMR, Proteus mirabilis, biofilm, gene expression.

1. Introduction

Loquat (*Eriobotrya japonica*) is a subtropical evergreen fruit tree from the Rosaceae family, native to southeastern China. Loquat had a long history of medicinal use in folk medicine **[1].** Furthermore, previous researchers have proved the strong antioxidant properties of various loquat extracts. Among 56 studied Chinese plants, loquat leaves showed higher antioxidant capacity than 54 other medicinal plants **[2].** In addition, loquat is considered one of the rich sources in terpenoids and flavonoids. The main identified triterpenoids were tormentic, ursolic, and oleanolic acids. While, the flavonoids were quercetin, naringenin, kaempferol 3-O-*β*-glucoside, and quercetin 3-O-*α*-rhamnoside. Some of these compounds have antioxidant, antitumor, antibacterial and antidiabetic properties **[3, 4].** The sesquiterpene glycoside isolated from loquat leaves had remarkable anti- hyperglycemic effect **[1].**

Urinary tract infections (UTIs) are common hospital-acquired infections. *Proteus mirabilis* is considered one of the most common pathogenic bacterium that induce UTI **[5].** Unfortunately, multi-drug resistant (MDR) strains of *P. mirabilis* are widespread globally **[6].** UTIs caused by *P. mirabilis* are often related with urinary stone formation and long-term catheterization **[7].** Among various *P. mirabilis* virulence factors, biofilm formation plays a significant role in its ability to cause recurrent and antibiotic-resistant UTIs **[8, 9].**

Recent efforts have focused on discovering new antibacterial and antibiofilm compounds. Natural sources like plant extracts and their phytoconstituents are valuable resources for combating multidrug-resistant bacteria **[10].** Phytoconstituents have antibacterial properties, and can inhibit bacterial adhesion to surfaces, and diminish the quorum sensing (QS) **[11].** Bacteria employ QS to control and regulate various functions, comprising virulence as well as biofilm formation **[12].**

Thus, this research paper was undertaken to evaluate the effectiveness of the two major compounds oleanolic acid and rutin isolated from *E. japonica* leaves on clinical isolates of *P. mirabilis,* hypothesizes that rutin and oleanolic acid exert antibacterial effects by inhibiting biofilm formation and QS regulated genes in *P. mirabilis*.

2. Materials and methods

2.1. Chemicals

All used solvents in this study (methanol, petroleum ether, methylene chloride, ethyl acetate, n-butanol, acetone, acetonitrile, and dimethyl sulfoxide) were purchased from El-Nasr Company for pharmaceuticals in Egypt. The purification process of all solvents was done following the procedure outlined in reference **[13].**

*Corresponding author e-mail: hanim93@mans.edu.eg.; (Hanim A. Youssef).
Received date 03 March 2025; Revised date 28 March 2025; Accepted date 17 April 2025
DOI: 10.21608/ejchem.2025.365113.11382

Analytical thin layer chromatography (TLC) was performed using Merck 60 GF_{254} precoated aluminium sheets.
Chromatographic detection of compounds was performed using aluminium chloride and vanillin-sulfuric acid spray reagents, as described in **[14].**
Column chromatography was performed using normal silica gel G 60-120 microns (α-chemika, India) and sephadex LH-20 (Solar bio, China) through the wet method in a specific solvent.
Sulfuric acid, vanillin, aluminium chloride hexahydrate and Ciprofloxacin were purchased from El-Nasr Company for pharmaceuticals.
The used kits in polymerase chain reaction (PCR) were Miniprep kit (Agilent, USA), and cDNA synthesis kit (Enzynomics, Korea).
Muller-Hinton agar medium used in antibacterial study was purchased Merck
3-HPLC analysis was done at the faculty of pharmacy, Ain shams university, Egypt. Using the instrument (model LC-10 A, Schimadzu, Kyoto, Japan) with C_{18} reversed phase column (19*300mm), detection was performed at a wave–length ranging from 215 to 400 nm. Experimental parameters for analyzing were adapted from a previous publication **[15].**

2.2. Plant material

Eriobotrya japonica mature leaves, with a health potential claim, were collected from the experimental farm of the Faculty of Agriculture, Mansoura University, Egypt, during the flowering stage in April, 2020. Their identity was confirmed by Prof. Mahmoud M. Kassem from the Faculty of Agriculture, Mansoura University, Egypt. A specimen voucher (EJ-2020) is currently held in our laboratory.

2.3. Phytochemistry of *E. japonica*

2.3.1. Extraction and liquid-liquid partitioning

Eriobotrya japonica air dried leaves (5.00 kg) were pulverized into a coarse powder and extracted with 70% methanol (15L, 4 times) at room temperature till exhaustion. The homogenous filtrate was pooled and then concentrated under reduced pressure at 40˚C yielded a brown reddish residue (545.224 g). A portion of the dried alcoholic extract (450 g) was dissolved in a minimal volume of methanol and distilled water (350mL), then successively fractionated with petroleum ether (600 mL, 5 times), methylene chloride (500 mL, 4 times), ethyl acetate (800mL, 6 times), and saturated n-butanol (500mL, 7 times). Each solvent was evaporated under reduced pressure at 40˚C and stored for further analysis.

2.3.2. Silica gel column chromatography for methylene chloride fraction

The methylene chloride fraction (20g) was loaded over silica gel column using petroleum ether with increased proportions of EtOAc up to 100% EtOAc, affording two sub fractions. Sub fraction I (165mg), was eluted by 20%EtOAc/petroleum ether and further purified by repeated crystallization from acetone afforded compound **1** (R_f = 0.76, on TLC using solvent system EtOAc/petroleum ether, 1:5, 100 mg).
Sub fraction II (775mg) was eluted by 30%EtOAc/petroleum ether. The pooled fractions were then evaporated under reduced pressure at 40˚C then re-chromatogrammed over silica gel column using petroleum ether and increased proportions of EtOAc up to 23% EtOAc, yielding compound **2** (R_f = 0.41, on TLC using solvent system EtOAc/methylene chloride, 1:5, 4 mg).

2.3.3. Silica gel column chromatography for EtOAc fraction

The EtOAc fraction (25g) was loaded over silica gel column with a gradient elution of petroleum ether and EtOAc up to 100% EtOAc, resulting in three sub fractions.
Sub fraction I (187mg) was eluted by 10%EtOAc/petroleum ether, then further purified over silica gel column with a gradient elution of methylene chloride and acetone up to 10% acetone, yielding compound **3** (R_f = 0.66, on TLC using solvent system EtOAc /methylene chloride, 1:5, 6 mg) and compound **4** (R_f = 0.48, on TLC using solvent system EtOAc /methylene chloride, 1:5, 10 mg).
Sub fraction II (94 mg) was eluted by 20%EtOAc/petroleum ether. The pooled fractions were dissolved in minimum volume of methanol and loaded onto the top of sephadex LH-20 column , that was previously packed and eluted using methanol, affording compound **5** (R_f = 0. 51, on TLC using solvent system EtOAc /methylene chloride 1:1, 13 mg).
Sub fraction III (138 mg) was eluted by 50%EtOAc/petroleum ether and purified preparatively on a C_{18} reversed-phase column using a solvent system of acetonitrile: water in a gradient elution. The gradient elution started with 15% acetonitrile and increased to 75% acetonitrile, resulting in the isolation of compound **6** (Rt 27.33 min, R_f = 0.41, on TLC using solvent system methanol/EtOAc, 1:19, 28 mg).

2.3.3. Characterization of isolated compounds

The separated compounds (**1-6**) were structurally characterized using proton nuclear magnetic resonance (1H-NMR), attached proton test (APT), and heteronuclear multiple bond correlation (HMBC) using NMR Bruker 400 MHz in a suitable solvent with tetramethylsilane (TMS) as an internal reference. Compound's structures are shown in (Fig.1).

Oleanolic acid (1)

Oleanolic acid (100mg) was isolated as a white powder. The ^{1}H -NMR spectrum (400 MHz, $CDCl_3$) ppm, showed signals at δ H 5.18(1H, *m*, H-12, C=C), 3. 59 (1H, *d*, *J* = 8 Hz, H-3, OH), 0.99(3H, *s*, H-23), 0.73 (3H, *s,* H-24), 0. 92(3H, *s,* H-25), 0.81(3H, *s,* H-26), 1.16(3H, *s,* H-27), 0.88(3H, *s*, H-29) and 0.86(3H, *s*, H-30). The APT spectrum (100 MHz, $CDCl_3$) displayed resonance for 30 carbons discriminated into one carbonyl at δ 178.7(C-28), two olefinic carbons at δ 121.9(C-12) and 144.3(C-13), and one oxygenated carbon at δ 77.3(C-3). The other carbon signals resonating in the range from δ 15.5 to 52.8 as follows: 52.8 (C-5), 47.2 (C-9), 46.1 (C-17), 45.9 (C-19), 42.1 (C-14), 41.7 (C-18), 39.5 (C-8), 38.8 (C-4), 38.5(C-1), 37.00 (C-10), 33.7 (C-21), 33.1 (C-29), 32.8 (C-22), 32.5 (C-7), 30.6 (C-20), 28.0 (C-23), 27.6 (C-15), 27.4 (C-2), 26.00(C-27), 23.7 (C-30), 23.3 (C-16), 21.3 (C-11), 18.4 (C-6), 17.3 (C-26), 16.5 (C-24), and15.5 (C-25). The stereo chemistry of C-3was confirmed from ^{1}H-NMR spectrum which displayed a signal at δ3.59 (*d, J*=8 Hz) that confirmed the *β* configuration of C-3 **[16].**

Corosolic acid (2)

Corosolic acid (4mg) was isolated as a white powder. The ^{1}H -NMR spectrum (400 MHz, DSMO-d_6) ppm, appeared signals at δ H 5.18(1H, *d*, H-12, *J*= 12 Hz, C=C), 4.42 (1H, *s*, H-3, OH), and 4.31 (1H, *d*, *J* = 8 Hz, H-2, OH), along with seven singlet methyl groups (each 3H) at δ 0.71(H-29), 0.79(H-30), 0. 83(H-25), 0.89(H-27), 0.91 (H-24), 0.93(H-26), and1.06 (H-23), indicating the triternoidal nature of the compound.

The APT spectrum (100 MHz, DSMO-d_6) ppm, showed signals at δ177.3 (C-28), 138.4 (C-13), 123.5 (C-12), 83.2 (C-3), 67.5 (C-2), 53.8 (C-5), 51.9 (C-18), 47.8 (C-9), 47.2(C-17), 46. 5 (C-1), 41.6 (C-14), 40.4 (C-20), 39.4 (C-4), 39.6 (C-19), 38.7 (C-8), 38.00 (C-10), 36.6 (C-22), 33.6 (C-7), 30.8 (C-21), 29.5 (C-23), 27.5 (C-15), 23.4 (C-16), 23.00(C-27), 22.5(C-11), 21.3 (C-29).18.4 (C-6), 17.2 (C-24), 16.7 (C-26,30), and14.3 (C-25) **[17].**

***Trans*- cinnamic acid (3)**

Trans- cinnamic acid (6mg) was isolated as a white crystal. The ^{1}H-NMR spectrum (400MHz, CD_3OD) ppm, showed signals at δ 7.57 (*t*, H-2, 6), 7.38 (*t*, H-3, 5), 7.4(*s*, H-4), 6.5 (*d*, *J*=16Hz, H-7) and 7.66 (*d*, *J*=16Hz, H-8). The APT spectrum (100 MHz, CD_3OD) ppm, showed signals at δ 169.00 (C-9), 144.6 (C-7), 134.7(C-1), 130.3(C-4), 128.8(C-3, 5), and128.2(C-2, 6) **[18].**

***Trans*-sinapic acid (4)**

Trans-sinapic acid (10mg) was isolated as an off-white powder. The ^{1}H-NMR spectrum (400MHz, CD_3OD) ppm, showed signals at δ 7.01 (*s*, H-26), 7.51 (*d*, *J*=16Hz, H-7), 6.43 (*d*, *J*=16Hz, H-8) and 3.82(*s*, OCH_3, C-3, 5). The APT spectrum (100 MHz, CD_3OD) ppm, at δ showed signals 168.8 (C-9), 148.4(C-3, 5) 145.3 (C-7), 137.8(C-4), 125.1(C-1), 116.5 (C-8), 106.5 (C-2, 6), and 56.5(OCH_3, C-3, 5) **[19].**

Fisetin (5)

Fisetin (13mg) was separated as a yellow powder. The ^{1}H-NMR spectrum (400MHz, CD_3OD) ppm, showed signals at δ 7.87(*t,* H-5), 7.67(*d*, *J*= 4 Hz, H-6), 7.57(*d*, *J*=4 Hz, H-8), 6.81 (*d*, *J*= 8 Hz, H-2′,5′) and 7.55(*d*, *J*= 4 Hz, H-6′). The APT spectrum (100 MHz, CD_3OD) ppm, showed signals at δ 173.00 (C-4), 162.8 (C-7), 157.00 (C-9), 147.2 (C-2′), 146.1 (C-3′), 144.8(C-2), 126.5 (C-5),137.1 (C-3),122.9 (C-1′), 120.2(C-6′),116.2 (C-5′),114.8 (C-2′),114.5(C-6),114(C-10), and 101.5(C-8) **[20, 21].**

Rutin (6)

Rutin (28mg) was obtained as a yellow powder. The ^{1}H-NMR spectrum (400 MHz, DSMO-d_6) of compound 6 showed the characteristic signals of the quercetin skeleton: 6.41(*t*, H-6),6.22 (*s,* H-8),7.57(*d, J*= 4 Hz, H-2′,6′), 6.88(*d, J*= 8 Hz, H-5′),5.37 (*d, J*= 6.4 Hz, H-1″),3.74 (*d, J*= 8 Hz,H-6″),4.45(*d, J*= 16 Hz,H-1‴),3.63 (*d, J*= 12 Hz,H-5‴) and1.02(*d, J*= 8 Hz, H-6‴). The APT spectrum (100 MHz, DSMO-d_6) ppm, showed signals at δ 177.4(C-4), 164.6(C-7), 161.6 (C-5), 157.1(C-9),156.6 (C-2),148.8(C-4′),145.2(C-3′),133.7(C-3), 122.00(C-6′),121.6(C-1′),116.7(C-2′),115.2(C-5′),104.4(C-1″),103.4(C-10),101.6(C-1‴),101.2(C-6), 94.1 (C-8),76.8(C-5″),76.3(C-3″),74.8(C-4‴),74.5(C-2″),72.3(C-2‴),71.00(C-4″),70.6 (C-3‴),68.7(C-5‴), 67.4 (C-6″), and18.1(C-6‴) **[22, 23].**

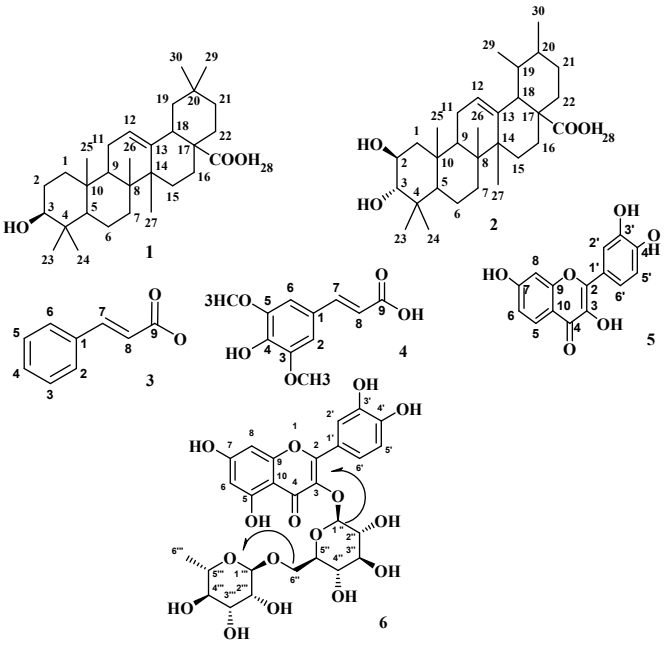

Figure 1: Chemical structure of compounds 1-6 isolated from *E. japonica* leaves

2.4. Antibacterial activity

2.4.1. *Proteus mirabilis isolates*

Thirteen clinical isolates of the tested bacteria were obtained from the culture collection of the Faculty of Pharmacy, Tanta University, Egypt.

2.4.2. Antibacterial effect

The antibacterial activity of the two major compounds (**1** and **6)** was tested using the agar well diffusion assay on Muller-Hinton agar plates at concentration of 1000 µg/mL as mentioned previously by **[24].** Bacterial suspensions were spread on the agar plate surfaces, and wells were punched out. The compounds were placed in the wells, with ciprofloxacin and dimethyl sulfoxide as positive and negative controls, respectively. After overnight incubation at 37°C for 24hrs the activity was evidenced by the presence of inhibition zones surrounding the well. Zones diameters were measured to evaluate the antibacterial activity of the studied compounds **[25].**

The minimum inhibitory concentrations (MICs) were revealed using a broth microdilution assay in microtitration plates **[26].** Concisely, the tested compounds were serially diluted and added to bacterial suspensions, followed by overnight incubation at 37°C. The MICs endpoint is lowest concentration at which no turbidity was observed, indicating antibacterial activity. The visual turbidity of the tubes, before and after the incubation was noted to confirm the MICs value [**27**].

2.4.3. Antibiofilm effect

The antibiofilm effect of the two major (**1** and **6**) was assessed as described by [**28**]. The optical density (OD) values were measured before and after the treatment with the tested compounds at 0.5MIC values. The capability to form biofilm was categorized into strong, moderate, weak, and non-biofilm as follow:

Non-biofilm former isolates (ODc < OD < 2ODc), weak biofilm former isolates (2ODc < OD < 4 ODc), moderate biofilm former isolates (4ODc < OD < 6ODc), and strong biofilm former isolates (6ODc < OD). The cut-off OD (ODc) was identified as the product of the addition of the mean OD to three standard deviation (SD) of the negative control **[29].**

2.4.4. Quantitative real-time PCR (qRT-PCR)

Compound **6** was evaluated for its efficacy on the gene expression of *mrpA*, *pmfA*, and *luxS* in *P. mirabilis* encoding QS and biofilm formation **[30].** Total RNA Miniprep kit was used for total RNA extraction and cDNA was produced-by TOPscript™ cDNA synthesis kit. Real-time PCR was done applying the Rotor-Gene Q 5plex (Qiagen, Germany) with primers recorded in Table S1 **[31].** The $2^{-\Delta\ \Delta CT}$ method was performed for calculating the gene expression fold change after the treatment **[32],** employing 16S rRNA as a housekeeping gene **[31].**

2.5. Statistical analysis

This research study was conducted on the basis of a completely randomized design (CRD) with three trails. The data was analyzed and expressed as mean ± standard deviation using CoStat Ver. 6.400 statistical data analytical software.

3. Results and discussion

3.1. Identification of compounds (1-6)

The methanol extract of *E. japonica* leaves was fractionated using petroleum ether, methylene chloride, ethyl acetate, and n-butanol. Two triterpenes identified as oleanolic acid (**1**) and corosolic acid (**2**) were isolated by column chromatography from the methylene chloride fraction and four compounds identified as: *tran*s-cinnamic acid (**3**), *trans*-sinapic acid (**4**), fisetin (**5**), and rutin (**6**) were isolated by column chromatography from the EtOAc fraction. Fisetin was isolated from this plant for the first time.

Compound **1** was separated as a white powder. The APT data displayed resonance for 30 carbon discriminated into one carbonyl at δ 178.7, two olefinic carbons at δ 121.9 and 144.3 and one carbinol methine carbon at δ 77.3, corresponding to one hydroxyl group at position 3. The other carbon signals resonated in the range from δ 15.5 to 52.8. The most denotive carbon signals were the two olefinic carbons at δ 121.9 and 144.3 for C-12, C-13, respectively, of the olean-12- ene triterpene and this was supported by the observation of a carbinol methine proton at δ H 3.59 (*d, J*=8 Hz, H-3) in the 1H-NMR spectrum, a feature of olean-12-ene triterpene. Moreover, the existence of an olefinic proton at δ H 5.18 (m, H-12) along with seven singlets of methyl groups from 0.73 to 1.16 ppm indicated that compound **1** was a triterpenoid **[33].** Additionally, the good compatibility of the NMR and the APT spectra of compound **1** matched well with those reported in a previous publication **[16],** confirming its structure as oleanolic acid previously isolated from *E. japonica* leaves.

Compound **2** was separated as a white powder. The APT data displayed resonance for 30 carbon atoms discriminated into one carbonyl at δ 177.3, two olefinic carbons at δ 123.5 and 138.4, and two carbinol methine carbons at δ 67.5 and 83.2, corresponding to one hydroxyl group at positions 2 and 3, respectively. The other carbon signals resonated in the range of δ 16.4 to 53.8. Seven methyl carbons appeared in the range of δ 16.7 to 29.5, affirmed by the ^{1}H-NMR data, in which they appeared as singlets each [(3H, *s*)] from δ 0.71 to 1.09. The data suggests that compound 2 is likely a member of the ursane type triterpene family. The ^{1}H-NMR spectroscopic data showed two hydroxy methine signals at δ 4.31 (H-2, *d, J*= 8 Hz) and 4.42 (H-3, s), along with one olefinic proton at δ 5.18 (*d, J*= 12 Hz). The stereochemistry of C-2 was affirmed from the ^{1}H-NMR spectrum, which displayed a signal at δ 4.31 (*d, J*= 8 Hz) indicating the *β*-configuration of C-2. The cumulative spectral information of compound **2** were in full agreement to those of corosolic acid **[17],** that was previously isolated from *E. japonica* leaves.

Oleanolic acid and corosolic acid are widespread triterpenes found together in many plants **[34].** Their spectroscopic data are similar, with the main variance being the positions of the methyl groups at C-29 and C-30. In oleanolic acid, the two groups are “geminally” attached to C-20, resulting in two protons attached to H-19, a characteristic sign of *β*-amyrins to which oleanolic acid belongs. On the other hand, in corosolic acid, the methyl groups of C-29 and C-30 are attached to C-19 and C-

20, respectively, making H-19 and H-20 to have one proton. Moreover, corosolic acid has an extra OH group at position 2, a characteristic sign of ursane type triterpenes to which corosolic acid belongs.

Compound **3** was obtained as white crystals. Five aromatic protons at δ_H (7.57*t*, H-2, 6), (7.38 *t*, H-3, 5) and (7.4*s*, H-4) indicating a monosubstituted aromatic ring were resonated in the ^{1}H-NMR spectrum. In addition, two doublets at δ 6.5 (H-7, *J*=16Hz) and 7.66 (H-8, *J*=16 Hz) confirming the presence of two *trans* -olefinic protons. The APT spectrum showed the presence of nine carbon signals, including two quaternary carbons and seven are methines (CH-).The carbon signal at δ 169.00 was assigned for C-9 of the carboxylic group. Additionally, two vinylic carbons at δ 118.3 (C-8), and 144.6 (C-7) also appeared in the APT spectrum.

Compound **3** was identified as *trans*- cinnamic acid, confirmed by the good compatibility of NMR data reported by **[18].** *Trans*- cinnamic acid has been previously isolated from *E. japonica.*

Compound **4** was separated as an off-white powder. The ^{1}H-NMR spectrum displayed resonance for two aromatic protons, at δ_H 7.01*s* (H-2, 6) indicating a tetrasubstituted aromatic ring bearing two methoxy protons at δ_H (3.82*s*). In addition, the signals at δ_H 7.51 (H-7) and 6.43 (H-8, *J*=16 Hz) indicating the presence of two *trans*-olefinic protons. Eleven carbons were appeared in the APT spectrum, nine of them assigned to the benzene ring bearing acrylic acid. The carboxylic carbon appeared at δ 168.8 (C-9), with four substituted aromatic carbons at δ_C 125.1(C-1), δ_C 148.8 (C-3, 5), and δ_C 137. 8 (C-4). The two unsubstituted aromatic carbons appeared at δ_C 106.5(C-2, 6). Additionally, two methoxy carbons at δ_C 56.5 (C-3′,5′) and two vinylic carbons at δ_C 145.3 (C-7), and 116.5 (C-8) were also observed in the APT spectrum.

Compound **4** was identified as 3, 5–dimethoxy-4- hydroxy *trans* -cinnamic acid (*trans*-sinapic acid), affirmed by the complete similarity to those reported by **[19].** This compound was previously isolated from *E. japonica.*

Compound **5** was isolated as a yellow powder. The ^{1}H-NMR spectra showed resonance at δ_H 6.81 (H-2′,5′, *dd*) and 7.55 (H-6′,*d*) suggesting the presences of an ABX-type aromatic system, which is distinctive for 3′, 4′-disubstituted B-ring in a flavonoid structure. An additional resonance at δ_H (7.87*t*, H-5) for mono hydroxylated A- ring in flavonoid skeleton was also observed. The APT spectra displayed resonance for fifteen carbon signals seven of them are oxygenated and the signal at δ_C 173.00 was assigned for C-4 of the flavonol skeleton **[35].** The aromatic carbon signals at 114.8, 116.2 and 120.2 ppm were assigned for C-2', C-5' and C-6', respectively cleared that the B- ring is disubstituted at positions 3′ and 4′ **[36].** From the ^{1}H-NMR spectra a signal resonated at δ_H 7.87*t* assigned for H-5 indicated that ring A is monosubstituted, and only position 7 is blocked by an OH group. This was further confirmed by the up filed shift of C-5 value at δ_C 126.5 confirming the absence of OH group at this position. The mentioned results of compound **5** were in agreement with previous studies on fisetin, which was isolated for the first time from *E. japonica* **[20, 21].**

Compound **6** was obtained as a yellow powder. The APT spectra assigned the presence of twenty-seven carbon signals, with fifteen typical of a flavonol skeleton **[35].** The remaining twelve signals (12C) were attributed to two sugar moieties, confirmed by anomeric doublets at δ 5.37 (1H, *d, J* = 6.4 Hz, H-1″) and 4.45 (*d, J* = 16 Hz, H-1‴). The absence of H-3 signal in the ^{1}H-NMR spectra and the existence of a signal at δ C 177.8 in the APT spectra assigned for C-4confirmed a flavonol nucleus with 3-OH substitution **[35].**

The oxygenation pattern of ring A was affirmed through the ^{1}H-NMR signals at δ 6.41 (*t*, H-6) and 6.22 (*s*, H-8), indicating that ring A is disubstituted at positions H-5 and H-7. As well as, the oxygenation pattern of ring B was affirmed through the ^{1}H-NMR signals at δ 7.57 (*d*, H-2′, H-6′), and 6.88 (*d*, H-5′), confirming that ring B is disubstituted at positions 3′ and 4′.

The stereo chemistry of C-1″was confirmed from ^{1}H-NMR spectrum which displayed a signal at δ 5.37 (*d*, *J*= 6.4 Hz) that confirmed the *β*- configuration of glucose moiety. While the *α* - configuration of the rhamnose moiety was confirmed by a signal at δ 4.45 (*d*, *J*= 16 Hz). In the HMBC spectrum, C-1‴ correlated with C-6″ of indicating a rutinosyl moiety. Besides, the glycosylation at C-3 was confirmed through the downfield resonance of C-2 at δ 156.6 and the up-field resonance of C-3 at δ 133.7 compared to published values for kaempferol (flavonol) in which C-2 resonates at δ 146.3 and C-3 at δ 136.1 **[37].** This was further confirmed from HMBC correlation in which the anomeric proton of glucose 5.37 (*d*, *J*= 6.4 Hz, H-1″) moiety is attached to C-3 of flavonol moiety (C-133.7). Compound **6** was identified as rutin, consistent with previous reports on *E. japonica* **[22, 23].**

3.2. Antibacterial action

The tested compounds (**1** and **6**) elicited inhibition zones around their wells as depicted in (Fig. 2). So, their MICs values were recorded employing the broth microdilution assay (Table1). Rutin manifested the highest activity with the lowest MIC values ranging from 32 to 128 µg/mL, against isolates Pr3 and Pr10. In contrast, oleanolic acid had the highest MIC value 2048 µg/mL against isolates Pr1, Pr3, Pr8 and Pr12.

The increased resistance against commercial antibiotics is a critical public health concern. *Proteus mirabilis*, a major uropathogenic bacterium, has developed resistance to numerous antibiotics along with its—multiple virulence factors **[38].** Therefore, there is a critical need to explore alternative options as a replacement for traditional antibiotics. Recently, a great focus on the potent antibacterial action of two dominant plant isolated compounds: flavonoids and terpenoids **[39].** These compounds have been shown to target the bacterial cell wall as the primary mechanism of action, while they are also affecting several biological functions, including the induction of the stress response **[40].**

Microbiological literature stated that flavonoids exhibit antibacterial effects through various mechanisms, including the suppression of nucleic acid synthesis, disabling the cytoplasmic membrane function, hindering the biofilm formation, and interaction with cell key enzymes **[41, 42].** Rutin, in particular, inhibits bacterial growth by targeting ATP-binding proteins **[43].**

These results are matching with previous literature reported that flavonoids have a promising effect in the upgrade of new antibacterial agents. Sometimes, the antibacterial activity of flavonoids was found to be up to 6-fold stronger than that of commercial antibacterial drugs **[44].** Oleanolic acid was reported to have a weaker antimicrobial effect against Gram-negative bacteria in previous studies **[45],** while flavonoids showed opposite tendency **[46].**

Previous studies **[47]** have also documented the antibiotic effect of terpenoids against many bacterial species. Their activity is more pronounced against Gram-positive bacteria compared to Gram-negative bacteria and ursolic acid being more potent than oleanolic acid.

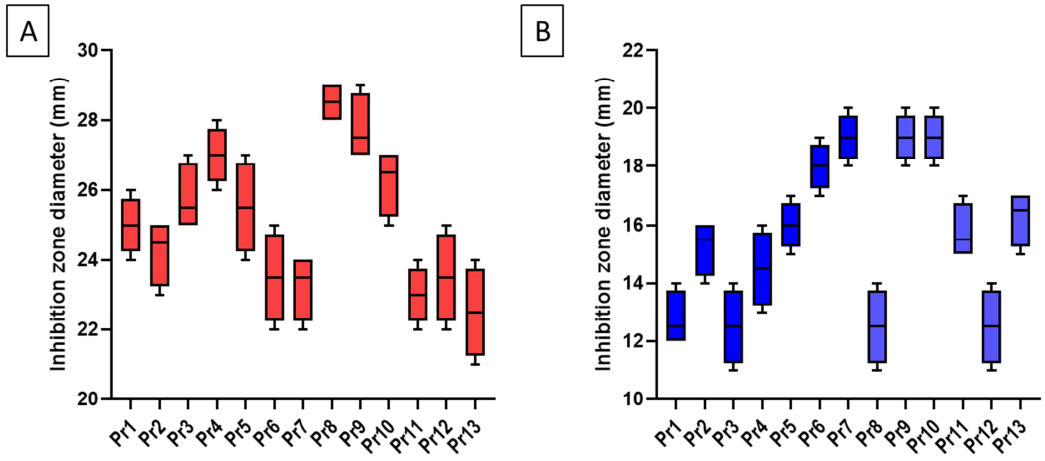

Figure 2: Inhibition zone diameters of A) rutin and B) oleanolic acid against *P. mirabilis* isolates.

Table 1: Minimum inhibitory concentrations of the tested compounds

Isolate code	Rutin	Oleanolic acid
Pr1	64	2048
Pr2	64	1024
Pr3	32	2048
Pr4	64	1024
Pr5	64	1024
Pr6	128	512
Pr7	128	512
Pr8	64	2048
Pr9	64	512
Pr10	32	512
Pr11	128	1024
Pr12	128	2048
Pr13	128	1024

3.3. Antibiofilm potential

Biofilm is a structure that encloses bacterial cells of the same or different species attached to surfaces, both abiotic and biotic through extracellular polymeric substances **[48, 49].** These biofilms-enclosed cells often exhibit increased pathogenicity and multidrug resistance **[50].** Thus, antibacterial agents with antibiofilm properties can effectively target and fight these hardy bacterial groups.

Rutin demonstrated antibiofilm action as realized by crystal violet assay. Figure S1 illustrates a reduction in the number of strong and moderate biofilm-forming isolates from 76.92% (ten isolates) to 23.08% (three isolates) when treated with rutin. In contrast, oleanolic acid did not show any antibiofilm action.

Our findings are in accordance with previous study **[51],** reported that oleanolic acid can inhibit the growth of biofilms produced by cariogenic bacteria, such as *Streptococcus mutans*, suggesting its probable use as an antibacterial drug against dental caries. Additionally, quercetin at a concentration of 80µg/mL has been shown to significantly reduce biofilm formation of the foodborne pathogen *Klebsiella pneumoniae*, as reported by **[52].** Furthermore, both naringenin and quercetin were able to prohibit the biofilm formation by *E. coli* O157:H7, as noted by **[53].** Early study verified that, the exposure of *S. aureus* RN4220 and *S. aureus* SA1199B to sub-MICs of flavonoids (hesperetin, phloretin, and myricitrin) caused a disturbance of the efflux system function in cells consequently, reduce their ability to produce biofilms **[54]**.

The mechanism of rutin in inhibiting biofilm formation was assessed through a growth kinetics assay, which demonstrated that rutin did not significantly reduce biomass. Therefore, this suggests that the reduction in cell number is not the primary factor affecting biofilm formation. Pathogens produce exopolysaccharides, which contribute to increase drug resistance. Exopolysaccharides protect bacteria biofilm through forming multiple layers enveloping the cell **[55].** Thus, interfering with exopolysaccharide production may be destroy the formed biofilm and also decrease the resistance of sessile cells **[56].**

3.4. qRT-PCR

The qRT-PCR obtained results approved the downregulate of gene expression (*mrpA, pmfA and luxS*) in seven isolates after rutin treatment, as shown in (Fig. 3). These genes play a vital role in biofilm and QS in *P. mirabilis* **[30].** These genes encode

various proteins that are involved in the communication between cells, adherence to surfaces and attachment **[57].** The *luxS* gene is important in the QS system that is a mechanism for interspecies communication by which bacteria can regulate diverse vital processes and genes, involved in biofilm formation **[57].** The possible effect of rutin has been found to promote metabolite production and suppress gene expression **[58].**

The study of **[43]** hypothesized that rutin possibly downregulate gene expression through inducing changes in ethanolamine metabolism, biotin biosynthesis and ATP-binding cassette related genes.

The changes in the expression of DEGs genes in *Xanthomonas oryzae* was observed after kaempferol addition using qRT-PCR analysis. The relative expression of important DEGs associated with the energy metabolism (GM002814, GM002906, GM004831), secretion system (GM003828, GM000092) and QS (GM003828, GM003065) were significantly downregulated, which emphasizes the validity flavonoids as a strong antibacterial agents **[59]**, which support the current findings.

These results provide visions into the influence of rutin on biofilm formation in *P. mirabilis* isolates, offering potential strategies for infection control and new drug development.

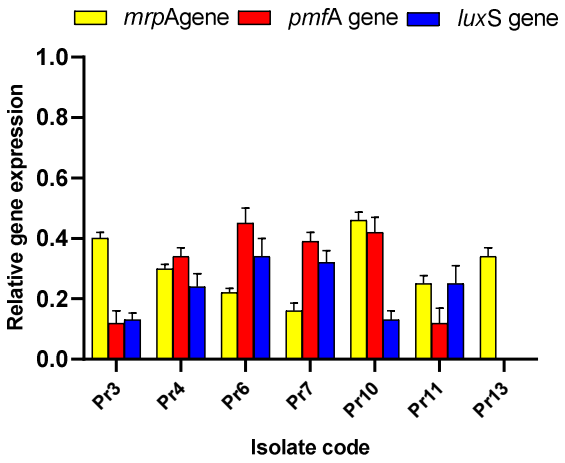

Figure 3: Bar graph demonstrating the downregulating consequence of rutin on the gene expression fold of the biofilm and QS genes in *P. mirabilis* isolates.

Conclusion

From *E. japonica* fractions, six compounds were isolated including two triterpenes [oleanolic acid (**1**), and corosolic acid (**2**)] from the methylene chloride fraction. Two phenolic derivatives [cinnamic acid (**3**), and sinapic acid (**4**)] and two flavonoids [fisetin (**5**), and rutin (**6**)] from the EtOAc fraction. By means of NMR and by comparison with reported data the structure of these compounds was established. To the best of our knowledge compound**5** has been identified from this plant for the first time. The two major compounds were examined *in vitro* as antibacterial agents. Rutin demonstrated significant antimicrobial efficacy against *P. mirabilis* isolates that form strong and moderate biofilms, while oleanolic acid did not exhibit any activity in this regard. The antibiofilm mechanism of rutin was illustrated through the molecular level using qRT-PCR. Thence, combined research could still greatly expand the knowledge of flavonoids bioactivities, thus helping to take the next step towards clinical application of natural antibiotic.

Ethical approval

This article does not contain any experiments with human participants or animals performed by any of the authors.

Conflict of interests

The authors have not declared any conflict of interests.

Data availability

Data will be made available on request.

References

[1]. Ao, X.; Zhaoa, L.; Lüa, H.; Rena, B.; Wub, H.;Chena, J. and Lia, W. (2015): New sesquiterpene glycosides from the leaves of *Eriobotrya japonica*. Natural Product Communications. 10(7): 1145-1147.

[2]. Song, F. L.; Gan, R. Y.;Zhang, Y.; Xiao, Q.; Kuang, L. and Li, H. B. (2010):Total phenolic contents and antioxidant capacities of selected Chinese medicinal plants. International journal of molecular sciences. 11(6): 2362-2372.

[3]. Taniguchi, S.; Imayoshi, Y.; Kobayashi, E.; Takamatsu, Y.; Ito, H., Hatano, T. and Yoshida, T. (2002): Production of bioactive triterpenes by *Eriobotrya japonica* calli. Phytochemistry. 59(3): 315-323. doi: 10.1016/s0031-9422(01)00455-1.

[4]. Kim, S. H. and Shin, T. Y. (2009): Anti-inflammatory effect of leaves of *Eriobotrya japonica* correlating with attenuation of p38 MAPK, ERK, and NF-κB activation in mast cells. Toxicology *in vitro*. 23(7):1215-1219. doi: 10.1016/j.tiv.2009.07.036.

[5]. Zhou, Y.; Zhou, Z.; Zheng, L.; Gong, Z.; Li, Y.; Jin, Y. and Chi, M. (2023): Urinary tract infections caused by uropathogenic *Escherichia coli:* mechanisms of infection and treatment options. International journal of molecular sciences. 24(13): 10537. https://doi.org/10.3390/ijms241310537.

[6]. Li, Z.; Peng, C.; Zhang, G.; Shen, Y.; Zhang, Y.; Liu, C.and Wang, F. (2022): Prevalence and characteristics of multidrug-resistant *Proteus mirabilis* from broiler farms in Shandong Province, China. Poultry science. 101(4):101710.

[7]. Brauer, A. L.; Learman, B. S. and Armbruster, C. E. (2023): Differential contribution of hydrogen metabolism to *Proteus mirabilis* fitness during Single-Species and polymicrobial catheterized urinary tract Infection. Pathogens. 12(12): 1377. https://doi.org/10.3390/pathogens12121377.

[8]. Wasfi, R.; Hamed, S. M.; Amer, M. A.and Fahmy, L. I. (2020): *Proteus mirabilis* biofilm: development and therapeutic strategies. Frontiers in cellular and infection microbiology. 10: 546552. https://doi.org/10.3389/fcimb.2020.00414.

[9]. Milo, S.; Heylen, R. A.; Glancy, J.; Williams, G. T.; Patenall, B. L.; Hathaway, H. J. and Jenkins, A. T. A. (2021): A small-molecular inhibitor against *Proteus mirabilis* urease to treat catheter-associated urinary tract infections. Scientific reports. 11(1): 3726. https://doi.org/10.1038/s41598-021-83257-2

[10]. Abdallah, E. M.; Alhatlani, B. Y.; de Paula Menezes, R. and Martins, C. H. G. (2023): Back to Nature: Medicinal plants as promising sources for antibacterial drugs in the post-antibiotic era. Plants. 12(17): 3077. https://doi.org/10.3390/plants12173077.

[11]. Monte, J.; Abreu, A. C.; Borges, A.; Simões, L. C. and Simões, M. (2014): Antimicrobial activity of selected phytochemicals against *Escherichia coli* and S*taphylococcus aureus* and their biofilms. Pathogens. 3(2): 473-498. https://doi.org/10.3390/pathogens3020473.

[12]. Zhou, L.; Zhang, Y.; Ge, Y.; Zhu, X. and Pan, J. (2020): Regulatory mechanisms and promising applications of quorum sensing-inhibiting agents in control of bacterial biofilm formation. Frontiers in microbiology. 11. 589640. https://doi.org/10.3389/fmicb.2020.589640.

[13]. Vogel A. (1974). Text Book of Practical Organic Chemistry, 3rd ed., Lotignian Group ltd., London.

[14]. Akpalo, A. E.; Saloufou, I. K.; Eloh, K . and Kpegba, K. (2020): Wound healing biomolecules present in four proposed soft aqueous extractions of *Ageratum conyzoides* Linn. International Journal of Biological and Chemical Sciences. 14(2): 638-651. https://doi.org/10.4314/ijbcs.v14i2.26.

[15]. Fatima, S. F.; Ishtiaq, S.; Lashkar, M. O.; Youssef, F. S.; Ashour, M. L. and Elhady, S. S. (2022): Metabolic profiling of *heliotropium crispum* aerial parts using HPLC and FTIR and *in vivo* evaluation of its anti-ulcer activity using an ethanol induced acute gastric ulcer model. Metabolites. 12(8): https://doi.org/10.3390/metabo12080750.

[16]. Dais P.; Plessel R.; Williamson K. and Hatzakis E. (2017): Complete ^{1} H and ^{13} C NMR assignment and ^{31} P NMR determination of pentacyclic triterpenic acids. Analytical Methods. 9(6): 949-957.

[17]. Xu, S.; Wang, G.; Peng, W.; Xu, Y.; Zhang, Y.; Ge, Y.; Jing, Y. and Gong Z. (2019). Corosolic acid isolated from *Eriobotrya japonica* leaves reduces glucose level in human hepatocellular carcinoma cells, zebrafish and rats. Scientific Reports. 9: 1-13. DOI: https://doi.org/10.1038/s41598-019-40934-7.

[18]. Kalinowska, M.; Jwisiocka, R. and Lewandowski W. (2007): The spectroscopic (FT-IR, FT-Raman and ^{1}H, ^{13}C-NMR) and theoretical studies of cinnamic acid and alkali metal cinnamates. Journal of molecular structure. 834(836): 572 -580.

[19]. Sakushima, A.; Coşkun, M. and Maoka T. (1995): Sinapinyl but-3-enylglucosinolate from *Boreava orientalis*. Phytochemistry. 40(2): 483-485.

[20]. Boukhary R.; Aboul-ElA M.; Al-Hanbali O. and El-Lakany A. (2017): Phenolic compounds from *Centaurea horrida* L growing in Lebanon. International Journal of Pharmacognosy and Phytochemical Research. 9(1): 1-4. DOI number: 10.25258/ijpapr.v9i1.8031.

[21]. Tsunekawa, R.; Hanaya, K.; Higashibayashi, S. and Sugai, T. (2018): Synthesis of fisetin and 2′,4′,6′-trihydroxydihyrochalcone 4′-O-*β*-neohesperidoside based on site-selective deacetylation and deoxygenation. Bioscience, Biotechnology and Biochemistry. 82(8): 1316-1322.

[22]. Șerban, G.; Pop, I A.; Horvath T. and Bota S. (2016): The isolation and identification of rutin from pharmaceutical products. Analele Universității din Oradea, Fascicula: Ecotoxicologie, Zootehnie și Tehnologii de Industrie Alimentară .109-114.

[23]. Selvaraj, K.; Chowdhury, R. and Bhattacharjee, C. (2013): Isolation and structural elucidation of flavonoids from aquatic fern azolla microphylia and evaluation of free radical scavenging activity. International Journal of Pharmacy and Pharmaceutical Sciences. 5: 743-749.

[24]. Attallah, N. G.; Al-Fakhrany, O. M.; Elekhnawy, E.; Hussein, I. A.; Shaldam, M. A.; Altwaijry, N.and Negm, W. A. (2022): Anti-biofilm and antibacterial activities of *Cycas* media R. Br secondary metabolites: *In silico*, *in vitro*, and *in vivo* approaches. Antibiotics. 11(8): 993. https://doi.org/10.3390/antibiotics11080993.

[25]. Abdelaziz, A.; Sonbol, F.; Elbanna, T. and El-Ekhnawy, E. (2019). Exposure to sublethal concentrations of benzalkonium chloride induces antimicrobial resistance and cellular changes in *Klebsiellae pneumoniae* clinical isolates. Microbial Drug Resistance. *25*(5): 631-638. https://doi.org/10.1089/mdr.2018.0235.

[26]. El-Banna, T.; Abd El-Aziz, A.; Sonbol, F. and El-Ekhnawy, E. (2019): Adaptation of *Pseudomonas aeruginosa* clinical isolates to benzalkonium chloride retards its growth and enhances biofilm production. Molecular biology reports. 46: 3437-3443.

[27]. Elekhnawy, E. A.; Sonbol, F. I.; Elbanna, T. E. and Abdelaziz, A. A. (2021): Evaluation of the impact of adaptation of *Klebsiella pneumoniae* clinical isolates to benzalkonium chloride on biofilm formation. Egyptian Journal of Medical Human Genetic*s*. 22:1-6.

[28]. Elekhnawy, E.; Sonbol, F.; Abdelaziz, A. and Elbanna, T. (2021): An investigation of the impact of triclosan adaptation on *Proteus mirabilis* clinical isolates from an Egyptian university hospital. Brazilian Journal of Microbiology. 52: 927-937.

[29]. Binsuwaidan, R.; Sultan, A. A.; Negm, W. A.; Attallah, N. G.; Alqahtani, M. J.; Hussein, I. A. and Elekhnawy, E. (2022): Bilosomes as nanoplatform for oral delivery and modulated *in vivo* antimicrobial activity of lycopene. Pharmaceuticals. 15(9): 1043. https://doi.org/10.3390/ph15091043.

[30]. Mirzaei, A.; Nasr Esfahani, B.; Ghanadian, M. and Moghim, S. (2022): Alhagi maurorum extract modulates quorum sensing genes and biofilm formation in *Proteus mirabilis*. Scientific Reports. 12(1): 13992. https://doi.org/10.1038/s41598-022-18362-x.

[31]. Rao, X.; Huang, X.; Zhou, Z. and Lin, X. (2013): An improvement of the 2ˆ (–delta delta CT) method for quantitative real-time polymerase chain reaction data analysis. Biostatistics, bioinformatics and biomathematics. *3*(3): 71-85.

[32]. Murray, C. J.; Ikuta, K. S.; Sharara, F.; Swetschinski, L.; Aguilar, G. R.; Gray, A. and Tasak, N. (2022): Global burden of bacterial antimicrobial resistance in 2019: a systematic analysis. The lancet. 399(10325):629-655.

[33]. Willow, L. (2011): Traditional herbal medicine research methods: identification, analysis, bioassay, and pharmaceutical and clinical studies. A John Wiley & Sons, Inc., Publication.

[34]. Xu, X.; Su, Q. and Zang, Z. (2012): Simultaneous determination of oleanolic acid and ursolic acid by RP-HPLC in the leaves of *Eriobotrya japonica* Lindl. Journal of Pharmaceutical Analysis.2: 238-240.

[35]. Agrawal, P.; Thakur, R. and Bansal M. (1989): Carbon-13 NMR of flavonoids. Elsevier Science Publishing Company INC.

[36]. Mikhaeil, B. R.; Badria, F. A.; Maatooq, G. T. and Amer, M. M. (2004): Antioxidant and immunomodulatory constituents of henna leaves. Zeitschrift für Naturforschung *C*. 59(7-8): 468-476.

[37]. Markham, K. R. and Ternai, B. (1976): ^{13}C- NMR of flavonoids—II: Flavonoids other than flavone and flavonol aglycones. Tetrahedron. 32(21): 2607-2612.

[38]. Mulani, M. S.; Kamble, E. E.; Kumkar, S. N.; Tawre, M. S.and Pardesi, K. R. (2019): Emerging strategies to combat ESKAPE pathogens in the era of antimicrobial resistance: a review. Frontiers in microbiology. 10: 1-24. https://doi.org/10.3389/fmicb.2019.00539.

[39]. Cushnie, T. P.and Lamb, A.J. (2011). Recent advances in understanding the antibacterial properties of flavonoids. International Journal of Antimicrobial Agents .38: 99–107.

[40]. Grudniak, A.M.; Kurek, A.; Szarlak, J.and Wolska, K.I.(2011): Oleanolic and ursolic acids affect the expression of the cysteine regulon and stress response in *Escherichia coli*. Current Microbiology. 62: 1331–1336.

[41]. Barbieri, R.; Coppo, E.; Marchese, A.; Daglia, M.; Sobarzo-Sánchez, E.; Nabavi, S.F.and Nabavi, S.M. (2017): Phytochemicals for human disease: An update on plant-derived compounds antibacterial activity. Microbiology Research. 196: 44–68

[42]. Górniak, I.; Bartoszewski, R. and Króliczewski, J. (2019): Comprehensive review of antimicrobial activities of plant flavonoids. Phytochemistry Reviews. 18: 241–272.

[43]. Wang, Z.; Shen, W.; Li, Y.; Wang, X.; Xu, G.; Yuan, X. and Wang, X. (2024): Integrated multi-omics analysis of *Klebsiella pneumoniae* revealed the discrepancy in flavonoid effect against strain growth between rutin and luteolin. bioRxiv. https://doi.org/10.1101/2024.02.20.581226.

[44]. Farhadi, F.; Khameneh, B.; Iranshahi, M. and Iranshahy, M. (2019): Antibacterial activity of flavonoids and their structure–activity relationship: An update review. Phytotherapy Research. 33(1): 13-40. https://doi.org/10.1002/ptr.6208.

[45]. Yoon, Y. and Choi, K.H. (2010): Identification of inhibitory effect on *Streptococcus mutans* by oleanolic acid. Life Science Journal. 20: 321–325.

[46]. Adamczak, A.; Ożarowski, M. and Karpiński, T. M. (2019): Antibacterial activity of some flavonoids and organic acids widely distributed in plants. Journal of clinical medicine. 9(1), 109. https://doi.org/10.3390/jcm9010109.

[47]. Jesus, J.A.; Lago, J.H.G.; Laurenti, M.D.; Yamamoto, E.S. and Passero, L.F.D. (2015): Antimicrobial activity of oleanolic and ursolic acids: An Update. Evidence-based complementary and alternative medicine. https://doi.org/10.1155/2015/620472.

[48]. Schulze, A.; Mitterer, F.; Pombo, J. P.and Schild, S. (2021): Biofilms by bacterial human pathogens: Clinical relevance-development, composition and regulation-therapeutical strategies. Microbial Cell.8(2): 28. https://doi.org/10.15698/mic2021.02.741.

[49]. Muhammad, M. H.; Idris, A. L.; Fan, X.; Guo, Y.; Yu, Y.; Jin, X. and Huang, T. (2020): Beyond risk: bacterial biofilms and their regulating approaches. Frontiers in microbiology. 11: 928. https://doi.org/10.3389/fmicb.2020.00928.

[50]. Chitlapilly Dass, S. and Wang, R. (2022): Biofilm through the looking glass: A microbial food safety perspective. Pathogens. 11(3):346. https://doi.org/10.3390/pathogens11030346.

[51]. Zhou, L.; Ding, Y.; Chen, W.; Zhang, P.; Chen, Y. and Lv, X. (2013): The *in vitro* study of ursolic acid and oleanolic acid inhibiting cariogenic microorganisms as well as biofilm. Oral Diseases. 19: 494–500.

[52]. Gopu, V.; Meena, C.K. and Shetty, P.H.(2015): Quercetin influences quorum sensing in food borne bacteria: *In-vitro* and *In-silico* evidence. Plos One. https://doi.org/10.1371/journal.pone.0134684.

[53]. Vikram, A.; Jayaprakasha, G.K.; Jesudhasan, P.R.; Pillai, S.D. and Patil, B.S.(2010): Suppression of bacterial cell-cell signaling, biofilm formation and type III secretion system by citrus flavonoids. Journal of applied microbiology. 109:515-527.

[54]. Lopes, L. A. A.; dos Santos Rodrigues, J. B.; Magnani, M.; de Souza, E. L. and de Siqueira-Júnior, J. P. (2017): Inhibitory effects of flavonoids on biofilm formation by *Staphylococcus aureus* that overexpresses efflux protein genes. Microbial Pathogenesis. 107: 193-197. https://doi.org/10.1016/j.micpath.2017.03.033.

[55]. Bridier, A.; Briandet, R.;Thomas, V.and Dubois-Brissonnet, F.(2011): Resistance of bacterial biofilms to disinfectants: a review. Biofouling. 27: 1017–1032.

[56]. Al-Shabib, N. A.; Husain, F. M.; Ahmad, I.; Khan, M. S.; Khan, R. A. and Khan, J. M. (2017): Rutin inhibits mono and multi-species biofilm formation by foodborne drug resistant *Escherichia coli* and *Staphylococcus aureus*. Food control.79: 325-332. https://doi.org/10.1016/j.foodcont.2017.03.004.

[57]. Colquhoun, J. M.and Rather, P. N. (2020): Insights into mechanisms of biofilm formation in *Acinetobacter baumannii* and implications for uropathogenesis. Frontiers in cellular and infection microbiology. 10: 253. https://doi.org/10.3389/fcimb.2020.00253.

[58]. Wang, Z.; Ding, Z.; Li, Z.; Ding, Y.; Jiang, F. and Liu, J. (2021): Antioxidant and antibacterial study of 10 flavonoids revealed rutin as a potential antibiofilm agent in *Klebsiella pneumoniae* strains isolated from hospitalized patients. Microbial pathogenesis. 159: https://doi.org/10.1016/j.micpath.2021.105121.

[59]. Li, A. P.; He, Y. H.; Zhang, S. Y.and Shi, Y. P. (2022): Antibacterial activity and action mechanism of flavonoids against phytopathogenic bacteria. Pesticide Biochemistry and Physiology. 188: https://doi.org/10.1016/j.pestbp.2022.105221.